

Supplemental Information

The Influence of Thick Cathode Fabrication Processing on Battery Cell Performance

Dewen Kong †, Haijing Liu *,†, Si Chen and Meiyuan Wu

Battery R&D, Battery Cell and Pack, General Motors, Shanghai 201206, China;
dewen.kong@gm.com (D.K.);

si.chen@gm.com (S.C.); meiyuan.wu@gm.com (M.W.)

* Correspondence: helen.liu@gm.com

† These authors contributed equally to this work.

Table S1. Materials specifications of active materials from supplier's certificate of analysis (COA)

	Chemistry	¹ Particle size (μm)	Tap density (g/cm ³)	Surface Area (m ² /g)
NM75	LiNi _{0.75} Mn _{0.25} O ₂	3.0	2.4	0.74
Graphite	C	20.2	1.45	0.86

¹ D50 particles size

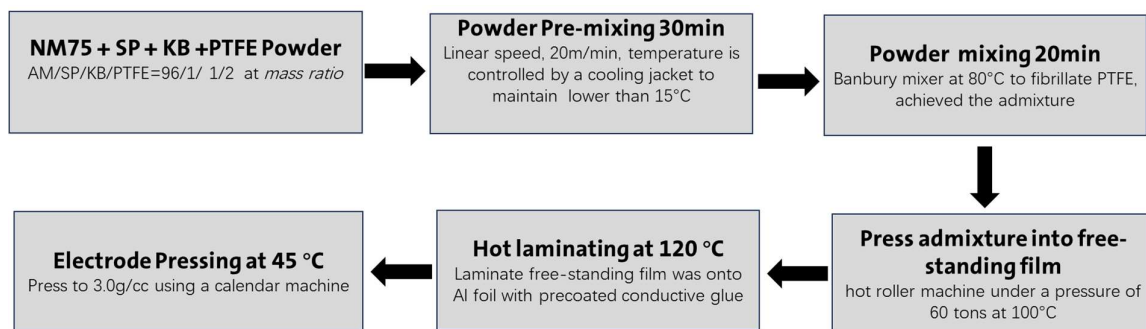


Figure S1. A scheme of F-NM75 electrode fabrication process.

Table S2. The formulations, mass loadings, and capacity loadings of F-NCMA, F-LMFP and F-graphite electrodes.

Electrode	Formulation at mass ratio, %	¹ Mass loading (mg/cm ²)	Capacity loading (mAh/cm ²)	Voltage range (V)
F-NM75	LMFP: SP: MWCNT: PTFE=96:1:1:2	31.9	4.7	2.5-4.3
F-NCMA	NCMA: SP: PTFE= 95.5:3.5:1	25.6	5.2	2.5-4.25
F-Graphite	Graphite: SP: CNT: PEO: PTFE=95.75:1: 1:1.25:1	16.42	5.2	0.01-2.0

¹ Single-sided mass loading.

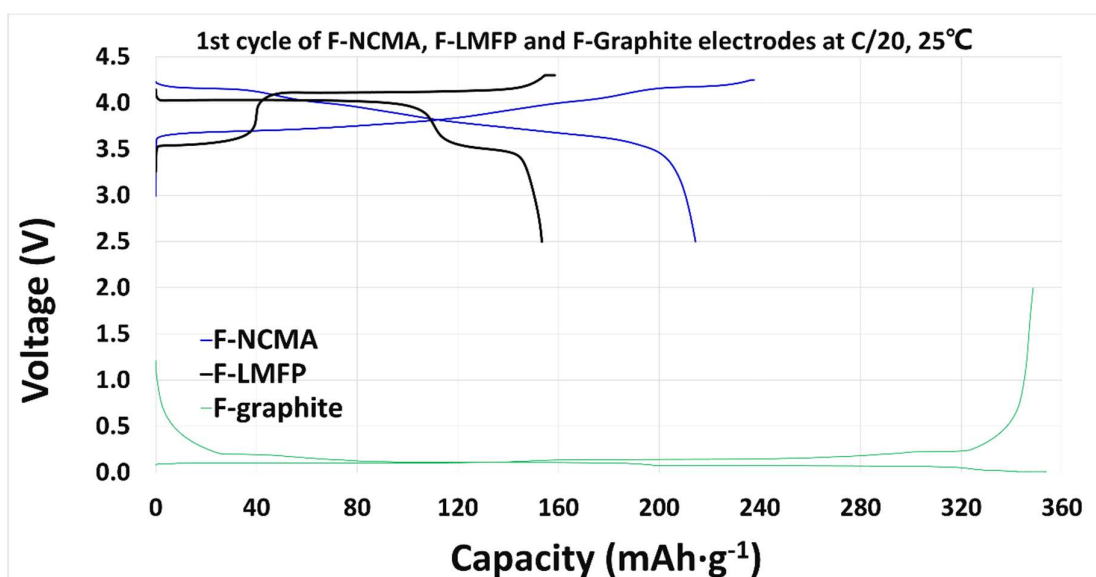


Figure S2. The charge and discharge curves of F-LMFP, F-NCMA and F-graphite electrode in half coin cells at C/20 at 25 °C.

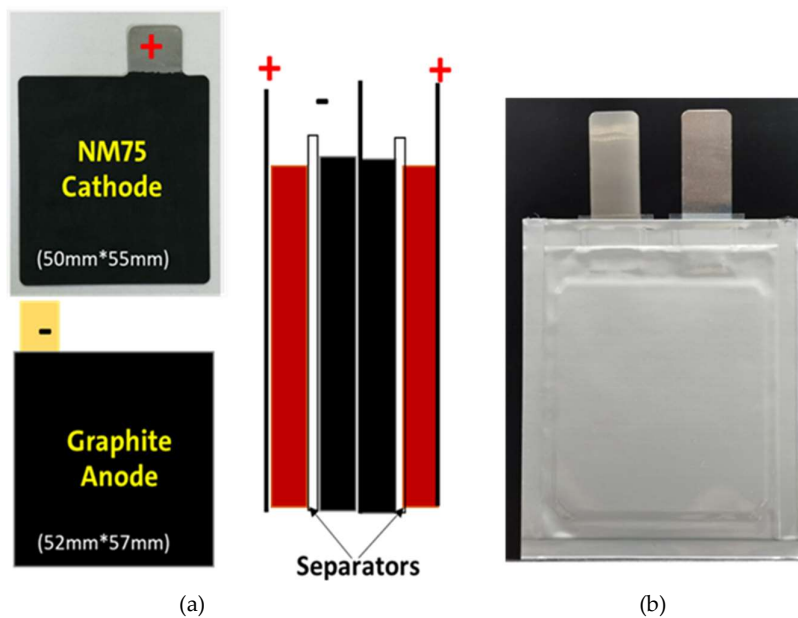


Figure S3. A schematic diagram (a) and image (b) of the NM75 || graphite bi-layer pouch cell.

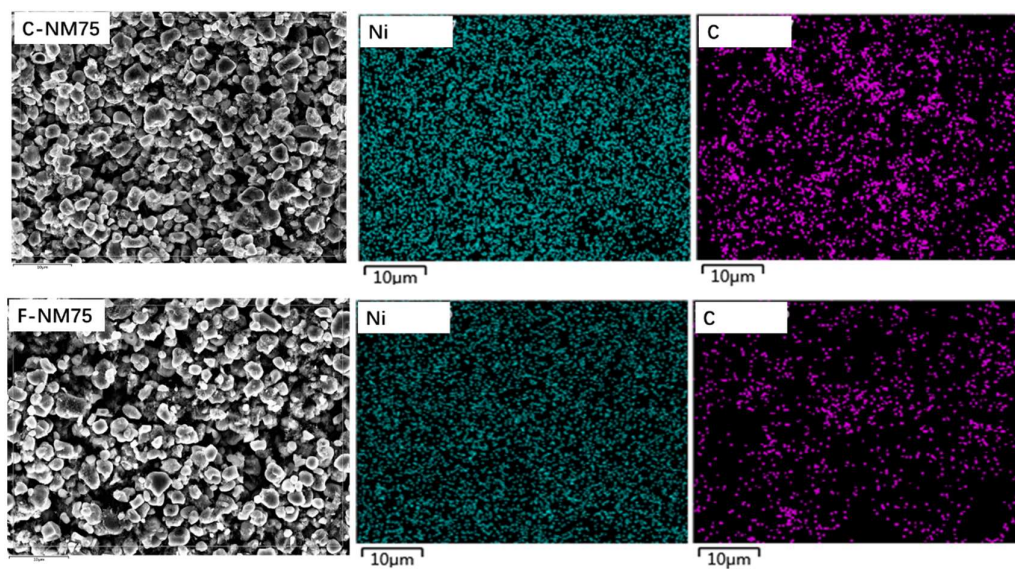
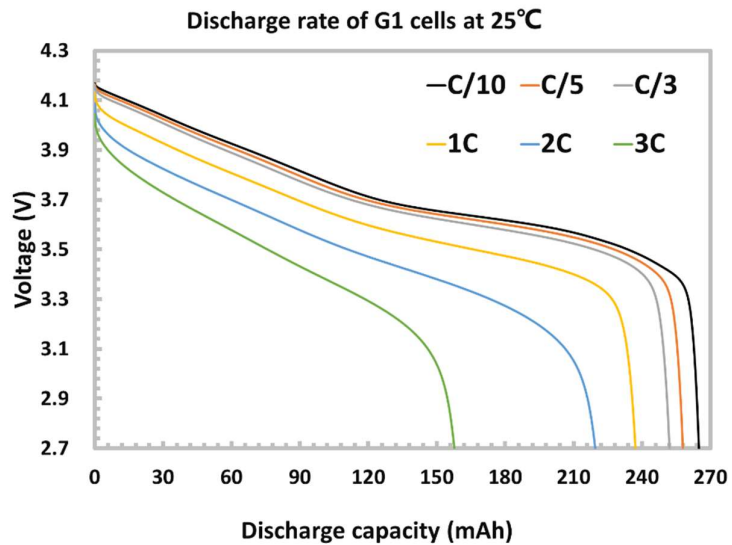
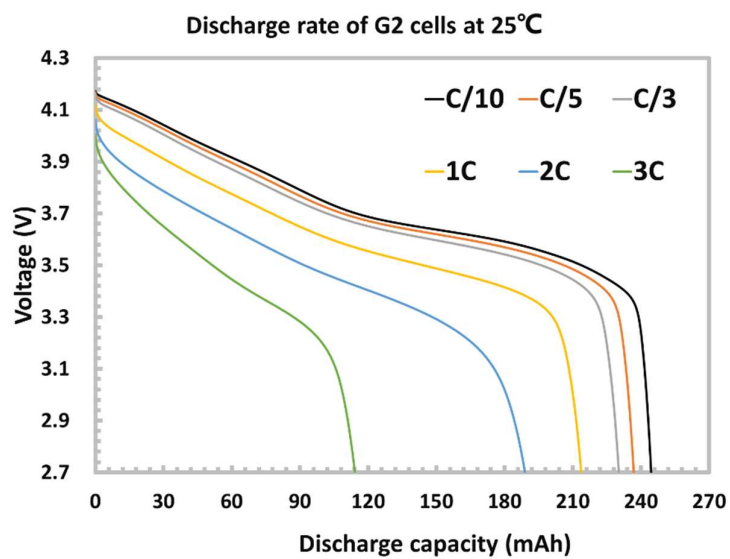


Figure S4. Comparison of the cross-section SEM and elemental mapping images of the NM75 electrodes.

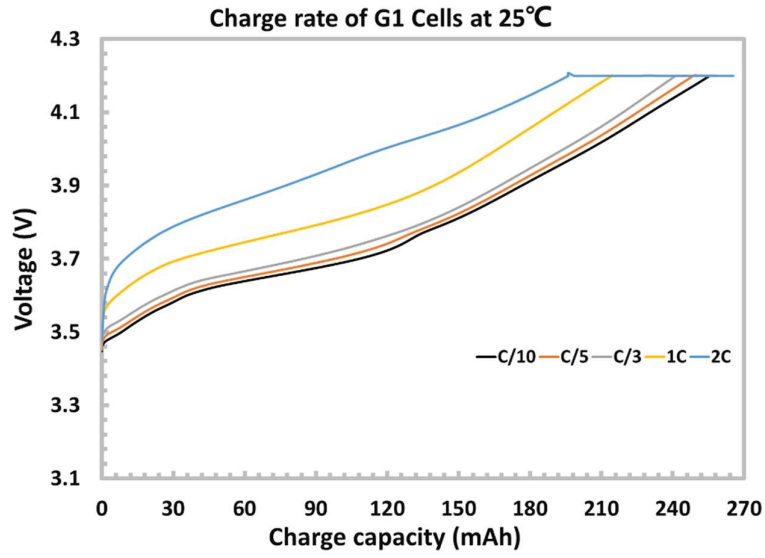


(a)

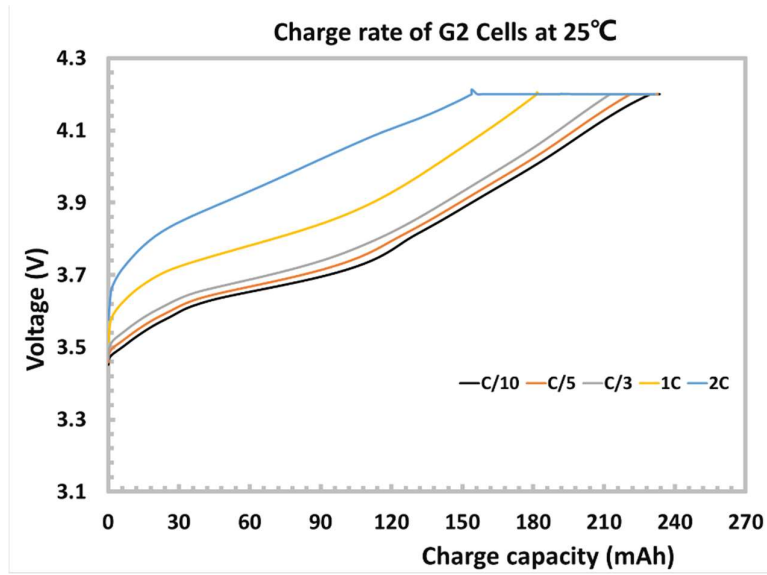


(b)

Figure S5. Voltage profiles of G1 (a) and G2 (b) in discharge rate test at 25 °C.



(a)



(b)

Figure S6. Voltage profiles of G1 (a) and G2 (b) in charge rate test at 25 °C.

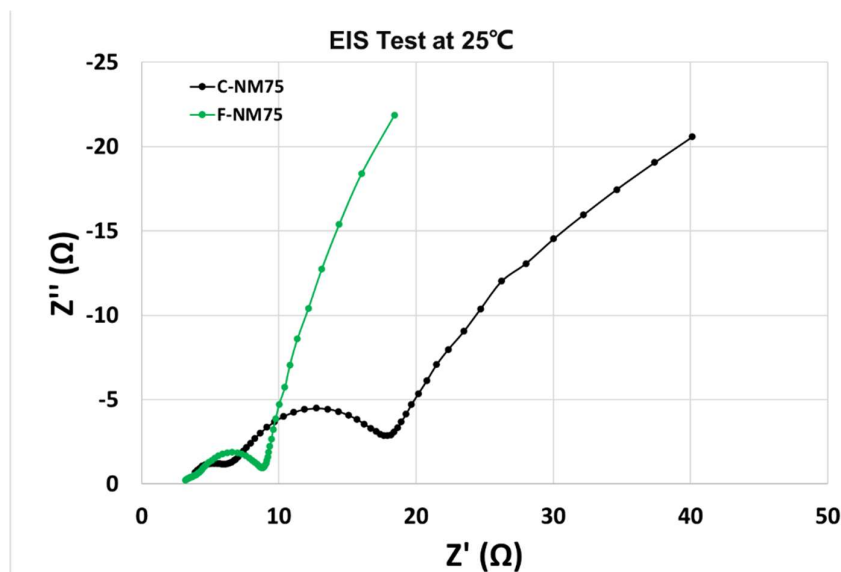


Figure S7. Nyquist plots of the NM75 electrodes.

Electrochemical impedance spectroscopy (EIS) measurements were performed on NM75 half coin cells using a Solartron cell test system (Solartron analytical 1470E) with frequency from 100000 to 0.01 Hz and an applied voltage amplitude of 5 mV. The Solartron system paired with a thermal chamber (Weissttechnik E series) to maintain 25 °C testing condition.

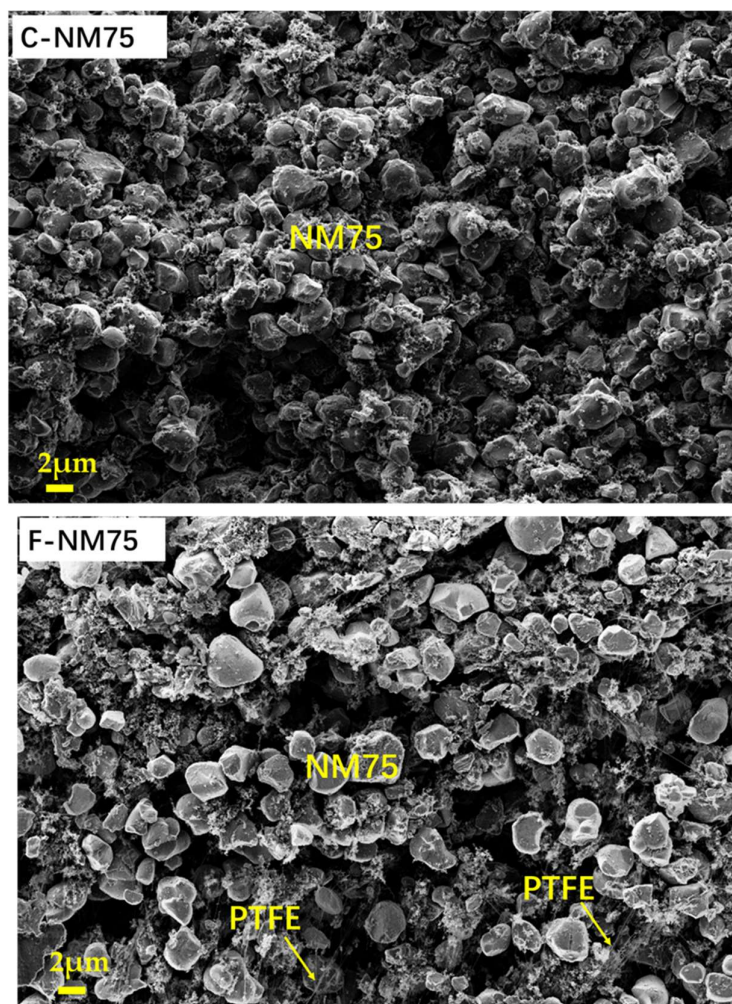


Figure S8. Lower magnitude cross-sectional SEM images of the NM75 electrodes.

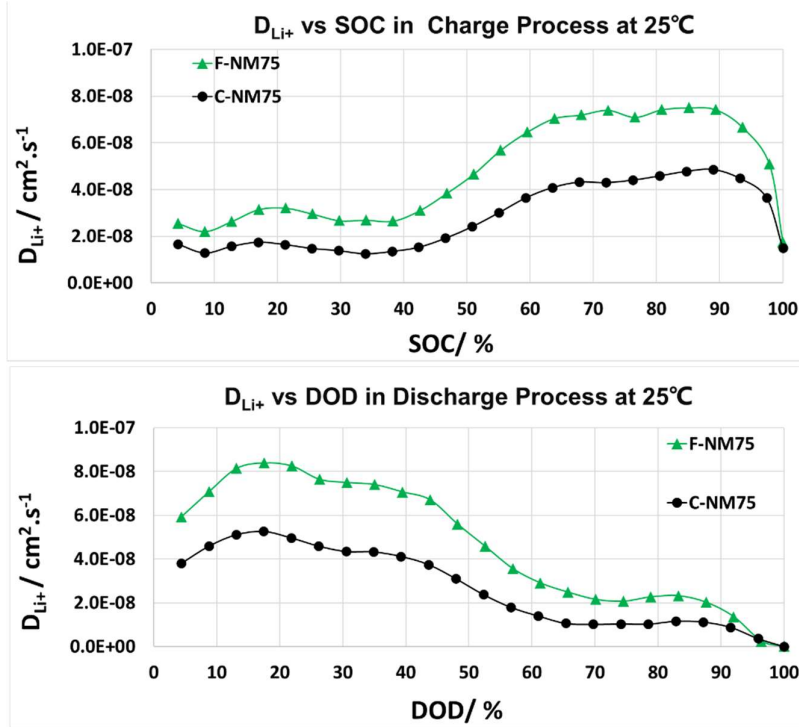


Figure S9. Calculated Li⁺ diffusion coefficient as a function of SOC and DOD 25 °C.

GITT measurements were performed in a battery cycler (Maccor, S4000) at room temperature. The assembled half coin cells with NM75 electrodes were tested between the voltage range 2.7 ~4.3 V with a two-hour break for relaxation, followed by a C/5 current pulse of 720 s duration. Two-hours rest and 720 s charge pulse were repeated until the voltage to 4.3 V (V_{max}). Both discharge and charge direction needed to be carried out to calculate the diffusion.

The diffusion coefficients of the NM75 electrodes are calculated based on the following equation [1].

$$D = \frac{4}{\pi\tau} \left(\frac{n_m V_m}{S} \right)^2 \left[\frac{\Delta E_S}{\Delta E_t} \right]^2$$

where S is the area of the electrode; n_m , V_m are the molar mass, and molar volume of the active material (NM75), respectively.

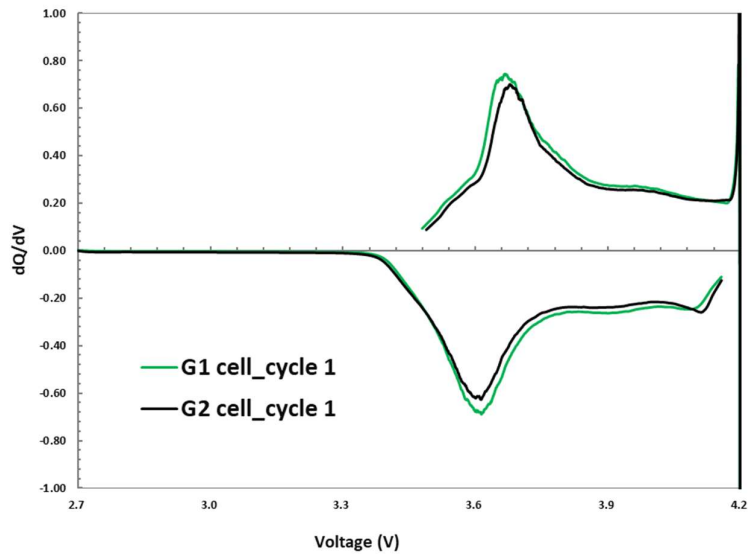
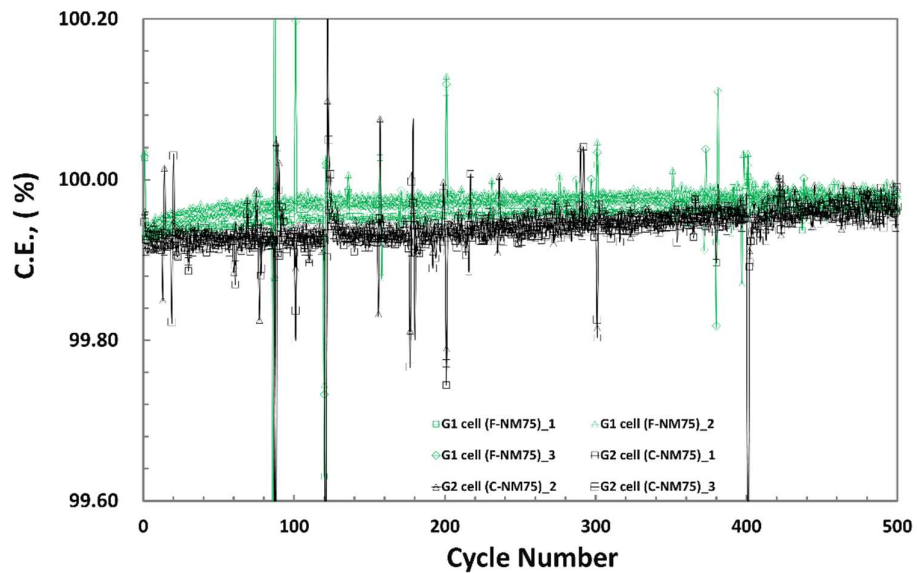
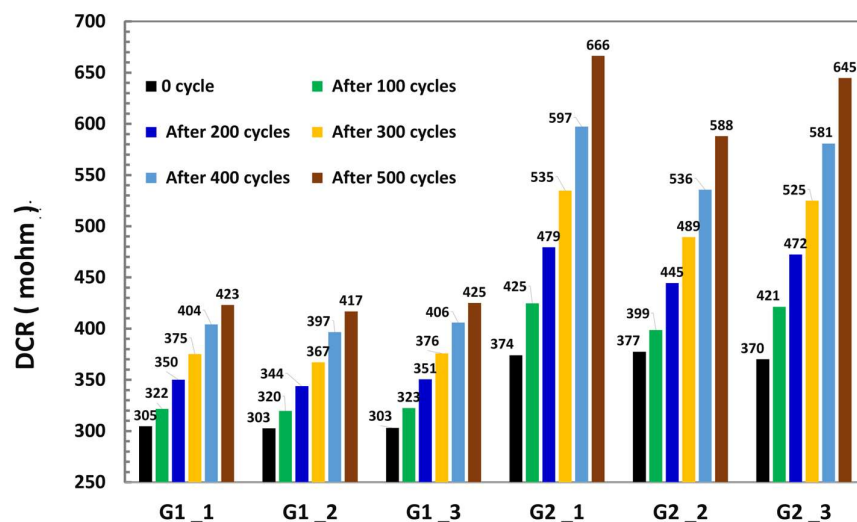


Figure S10. A differential capacity plot of G1 and G2 cells.



(a)



(b)

Figure S11. The coulombic efficiency (a) and DCR (b) of NM75||graphite pouch cells in the cycle life test at 25 °C.

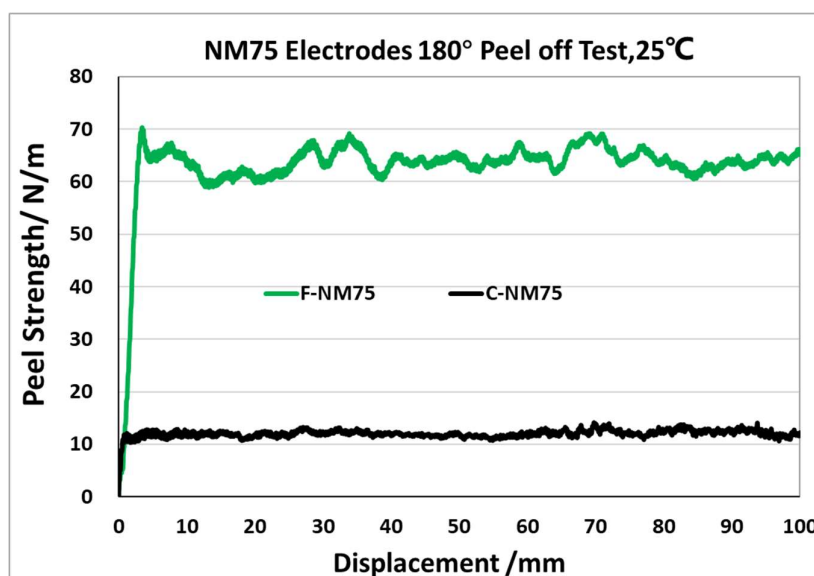


Figure Peeling strength/displacement curves in the 180° peel-off test of NM75 electrodes.

The off 180° peel test was used to verify the adhesive force of NM75 electrodes. The NM75 electrode's peel strength was measured on Shimadzu AGS-X under a 3 cm/min speed with a sample dimension of 2.5 cm*10 cm (W*L).

References

1. Ryu, M., Hong, YK., Lee, SY. Ultrahigh loading dry-process for solvent-free lithium-ion battery electrode fabrication. *Nat Commun.* 2023, 14, 1316.